


Article

# Analysis and Optimization of a Regenerative Snubber for a GaN-Based USB-PD Flyback Converter

Fabio Cacciotto <sup>1</sup>, Alessandro Cannone <sup>1</sup>, Emanuele Cassarà <sup>1,2</sup> and Santi Agatino Rizzo <sup>2,\*</sup> <sup>1</sup> ST Microelectronics s.r.l., 95121 Catania, Italy; fabio.cacciotto@st.com (F.C.); emanuele.cassara02@st.com (E.C.)<sup>2</sup> Department of Electrical Electronic and Computer Engineering (DIEEI), University of Catania, 95125 Catania, Italy

\* Correspondence: santi.rizzo@unict.it

**Abstract:** This paper presents a high-efficiency GaN-based 65 W Quasi-Resonant (QR) Flyback converter. The converter is characterized by a wide input voltage range and a variable output voltage, and it is designed as a Switch Mode Power Supply (SMPS) for high power density USB-Power Delivery (USB-PD) applications. To increase the efficiency and power density, a regenerative snubber clamp solution has been used to limit the excursion of the drain voltage during the power switch turn-off. The activity involved the modeling of the converter, the sizing of the regenerative snubber, and the design of the flyback transformer. Furthermore, a dedicated test application board was used to verify the effectiveness of the solution. The results were compared with those obtained using a flyback converter with an RCD snubber.

**Keywords:** efficiency; power electronics; Flyback; GaN



**Citation:** Cacciotto, F.; Cannone, A.; Cassarà, E.; Rizzo, S.A. Analysis and Optimization of a Regenerative Snubber for a GaN-Based USB-PD Flyback Converter. *Electronics* **2024**, *13*, 1045. <https://doi.org/10.3390/electronics13061045>

Academic Editors: Luis M. Fernández-Ramírez, Ahmed Abu-Siada, Jean-Christophe Crebier, Kai Fu, Zhiwei Gao and Eladio Durán Aranda

Received: 17 January 2024

Revised: 5 March 2024

Accepted: 6 March 2024

Published: 11 March 2024



**Copyright:** © 2024 by the authors. Licensee MDPI, Basel, Switzerland. This article is an open access article distributed under the terms and conditions of the Creative Commons Attribution (CC BY) license (<https://creativecommons.org/licenses/by/4.0/>).

## 1. Introduction

There is a large interest in improving the efficiency of Flyback converters, characterized by a wide input voltage range and a variable input and output voltage due to its wide applications [1–4]. To this aim, several non-dissipative clamp circuits, passive [5,6] and active [7–10], have been proposed and optimized over the years to limit the voltage spikes on the main switch, typically a power MOSFET, due to the transformer leakage inductance and optimized to not excessively affect the overall efficiency system [11]. A regenerative solution has been proposed in the work presented in [12] as an improvement of the non-dissipative passive LCD solution, replacing the snubber inductance with further winding in the transformer; this solution has been widely used in applications to increase the efficiency and power density of the converter [13].

However, the literature only reports studies in which the regenerative solution is designed for topologies characterized by a fixed DC output voltage. In most cases, also the input voltage of the converter is fixed to a certain value. A new integrated semi-active regenerative snubber that integrates the inductor into the main transformer to decrease the number of components thus reducing PCB size is presented in [9]. Partial coupling of a snubber inductor with a secondary side makes it possible to recover part of the transformer leakage energy directly to the secondary side to increase efficiency. However, only simulations are performed and fixed input and output voltage are considered. In the work presented in [12], the improvement in terms of efficiency with a regenerative solution was validated with a flyback prototype operating in Discontinuous Conduction Mode (DCM) supplied with a 150 V-DC input voltage and a fixed output voltage of 15 V-DC. Comparatively, in the work presented in [13], a regenerative snubber was designed for a MOSFET-based flyback converter, operating in Continuous Conduction Mode (CCM) with a fixed input voltage higher than 300 V-DC and a 24 V-DC output voltage. Moreover, the work presented in [13] also reports the main constraints that must be considered to size the regenerative clamp circuit, this allows us to obtain the equations to establish a range of

suitable parameters, which depends on the input and output voltage of the converter. In the work presented in [14], the state-plane approach is proposed to size the regenerative snubber reported in the work presented in [13]. A modified version of the regenerative solution is proposed in the research presented in [15], where the auxiliary winding is replaced with a separate transformer, allowing the leakage energy to be transferred directly to the output stage. An efficiency comparison for two different fixed input voltages (72 Vdc and 200 Vdc) is reported. However, compared with a conventional regenerative snubber, this solution only improves the converter's efficiency at low input voltage. For high input voltage, the modified version seems to be worse than the conventional one, as the efficiency is reduced.

In the work presented in [16], an efficiency comparison between energy regenerative and an RCD snubber for a Flyback single-stage isolated power-factor-corrected power supplies that operates in DCM was proposed. The comparison for fixed input (110 V-DC) and output voltage condition (28 V-DC) varying the output load (60–100 W) highlighted that the solution with regenerative clamping reaches better efficiency. Similarly, in the work presented in [17], a MOSFET based flyback converter with an energy regenerative snubber circuit was designed for a 35 V-DC input voltage and a 380 V-DC output voltage. In this case, an efficiency evaluation by varying the output power from around 25 W to 200 W was performed. The experimental results reported an efficiency improvement from 25 W to 100 W, but efficiency was decreasing over 100 W. Moreover, the actual improvement in a comparison with a passive snubber solution was not investigated. In the work presented in [18] the stability of a MOSFET-based Flyback converter with a regenerative energy snubber characterized by a fixed input voltage (311 V-DC) and 12 V-DC output voltage was studied. Simulation results were obtained by exploiting the PSIM software (version 2021b). The study has shown that the solution can be implemented without problems in their dynamics. In the work presented in [19], a series input parallel output interleaved flyback converter with regenerative leakage inductance energy has been proposed. Experimental results were performed in a prototype working in DCM and CCM, with a fixed input voltage (400 V-DC) and output voltage (24 V-DC). The regenerative solution resulted in high efficiency and power density compared to the series input parallel output interleaved flyback with RCD snubber.

A difference in the proposed converter is the adoption of a GaN-based transistor as the main switch rather than a MOSFET, thus increasing efficiency and reducing system size, weight and cost [20]. The proposed solution is an offline converter exploiting the GaN-based quasi-resonant flyback topology, that can be supplied with an input voltage in a range between 90 V-AC and 264 V-AC. An additional advantage in comparison with the previous works is obtained thanks to the use of a GaN switch because it enables working in quasi-resonant mode thus obtaining higher efficiency. In detail, this solution allows to drastically reduce the switching losses, so the converter meets a high efficiency compared with most of the applications present in the literature. It is worth noting that, the adoption of a GaN switch together with the possibility of working in quasi-resonant mode improves the converter efficiency also when a dissipative RCD snubber is used. In fact, the quasi-resonant operation mode allows to turn on the switch when the voltage across the device is low, that is operating in Zero Voltage Switching (ZVS), and the GaN based device presents a lower parasitic capacitance than a traditional MOSFET.

In the work presented in [21], a GaN-based device in a quasi-resonant converter is adopted to drastically reduce the switching losses and an efficiency comparison between the traditional RCD solution and the regenerative solution has been done but in an easier scenario, that is constant output voltage. A solution allowing to reach ZVS on the main switch was considered also in the work presented in [22], which adopted a regenerative snubber circuit for GaN-based low-power flyback converter. The snubber circuit recycled the leakage inductance energy and reduced the effect of parasitic loop inductance thanks also to the use of a low-side auxiliary switch. The analysis was experimentally validated with a prototype characterized by a fixed input (15 V-DC) and output voltage (5 V-DC). A

reduction in the peak voltage across the main switch with the snubber was reported but it lacks in a comparison with an RCD solution. A GaN switch was adopted also in the work presented in [23] where a novel regenerative snubber with both an additional inductor and an auxiliary winding in the transformer was presented. The power supply worked in CCM with two different input voltages (115 V and 230 V-AC) and the efficiency comparison with the conventional LC snubber solution and the traditional regenerative snubber for a fixed output voltage (12 V-DC) reported that the traditional regenerative solution allows to reach a higher efficiency for both input voltage compared to the proposed solution and the LC solution.

A first contribution of this paper is the concurrent adoption of wide input and output voltage. More specifically, differently from previous works, in this paper four output voltages between 5 V and 20 V, up to a maximum power of 65 W (20 V, 3.25 A) have been considered. Considering that the voltage at the input and the output of the converter are not fixed, another contribution in this work is the identification of a worst-case to size the regenerative snubber. In fact, all the previous works using GaN or MOSFET do not consider different input and output voltages. Therefore, this work investigates, for the first time, the challenge of sizing the regenerative snubber related to the worst-case in this kind of application. To this aim, a circuit simulation-based parametric analysis of the converter components has been executed to identify the values that maximize the converter performance.

It is worth noting that, although the adoption of a GaN switch and the related enabled possibility to work in resonant mode provide several advantages, different challenges have to be faced. In particular, a safe design of the maximum drain-source voltage of the GaN switch must be cared. When the MOSFET breakdown voltage is exceeded, the avalanche condition occurs thus causing an increase in the current flowing through the junction. This mechanism could not be destructive if timely countermeasures are executed. In the case of GaN, the avalanche condition is not possible and the safety limit is given by the absolute maximum rating (AMR). It is absolutely prohibited to overcome this limit because it causes failure. For all these reasons, in a GaN based converter, the snubber must be designed to surely guarantee that the drain-source voltage does not exceed the AMR, which, in turn, implies dissipating greater energy in the RCD snubber to avoid failure. Hence, the use of a regenerative solution in a GaN-based flyback converter even more could increase the efficiency.

Therefore, the work focuses on sizing and optimizing the components of the regenerative clamp circuit, that replaces the traditional dissipative RCD clamp. The goal is to properly handle the GaN switch and to obtain a higher efficiency compared with the efficiency obtained with the typical RCD solution. A new challenge that has been faced is reaching the objective regardless of the input voltage and the output profile, modifying the application board, in particular replacing only the clamp circuit and the transformer. A preliminary study was conducted by performing circuit simulations of the converter which required a proper initial modelling. This allowed us to study the behavior of the regenerative snubber in the entire input voltage range and for each profile. Based on the simulation results, the best size of the regenerative clamp and transformer design has been found. Finally, the new solution was compared with a traditional one, through a dedicated test bench. The results have shown that opportunely designing the regenerative snubber is possible to improve the efficiency for each output fixed profile of the converter even for wide-range input voltage applications, so efficiency can reach 94%.

## 2. The Regenerative Snubber

The Flyback topology is widely used for power converters, thanks to its simplicity and flexibility. As illustrated in Figure 1, it is characterized by a single power switch and a transformer used as an energy storage element that also provides electrical insulation. By properly controlling the switch commutations, the output voltage of the converter can be regulated.

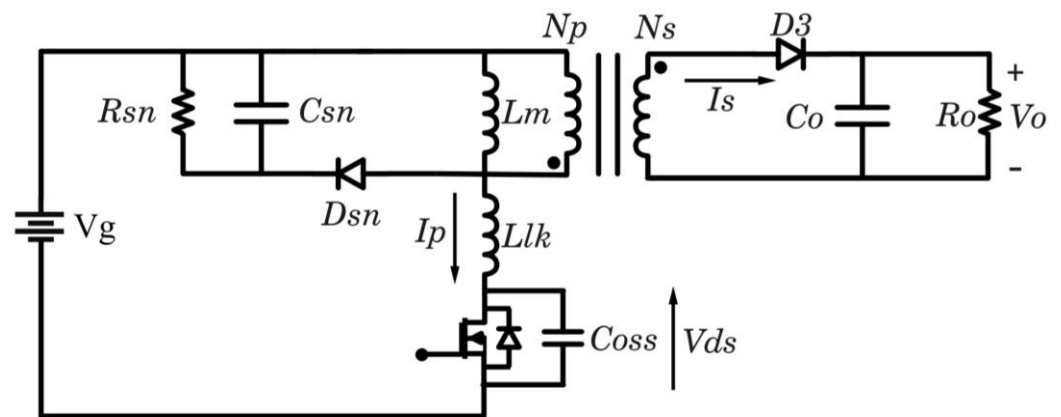


Figure 1. Flyback Converter with RCD snubber.

The flyback transformer is a two-coupled inductive magnetic component. It can be mainly represented by a primary inductance  $L_p$  that stores the energy during the switch on-state for subsequently transfers it to the secondary side through the transformer. However, part of the energy stored in the primary winding cannot be transferred to the secondary winding due to the flux from the primary winding, which does not perfectly couple to the secondary winding.

When the switch turns off, the transformer leakage inductance,  $L_{lk}$ , causes a voltage spike across the drain that might exceed the breakdown voltage of the switch itself, resulting in unsafe operations of the converter.

Therefore, a turn-off snubber was required to limit the peak voltage stress. In the schematic of Figure 1, is included one of the simplest circuitual solutions that allows the implementation of this snubber, also known as the RCD Snubber. With the RCD clamp approach, the leakage inductance energy is dissipated using a resistor. Due to the high-power dissipation, this dissipative snubber circuit cannot easily meet the efficiency requirements of modern power supplies. Many different improved flyback-based topologies have been developed, to reduce the inevitable switching losses, as well as the losses across the snubber.

The flyback topology efficiency improvement can be reached, thanks to a snubber circuit called Energy Regenerative Snubber. In detail, it recovers the leakage energy from the snubber capacitor to the DC bus, thus improving energy efficiency and power density. As shown in Figure 2, this clamp circuit consists of a couple of diodes,  $D1$  and  $D2$ , a capacitor  $C_{sn}$  and an extra auxiliary winding in the transformer.

The working principle is the following. When the power switch is turned-on,  $D2$  is forward biased and the snubber capacitance  $C_{sn}$  is discharged (Figure 2a). During this interval, the voltage across  $C_{sn}$  can be expressed as:

$$v_{C_{sn}}(t) = V_g \frac{N_r}{N_p} - \left( V_g \frac{N_r}{N_p} - v_{C_{sn}(max)} \right) \cos(\omega_0 t), \tag{1}$$

where:

$$\omega_0 = \frac{1}{\frac{N_r}{N_p} \sqrt{L_{lk} C_{sn}}} \tag{2}$$

The voltage  $v_{C_{sn}}(t)$  reaches the minimum at half of the resonance period:

$$v_{C_{sn}(min)} = 2V_g \frac{N_r}{N_p} - v_{C_{sn}(max)} \tag{3}$$

When the power switch is turned-off, the energy of the leakage inductance  $L_{lk}$  is transferred to  $C_{sn}$ , that clamps the maximum drain voltage of the switch. It is possible to prove that the voltage  $v_{Csn(max)}$  can be expressed as follows [13]:

$$v_{Csn(max)} = v_{Csn(min)} + I_m \sqrt{\frac{L_{lk}}{C_{sn}}}, \tag{4}$$

Therefore:

$$v_{Csn(min)} = V_g \frac{N_r}{N_p} - \frac{I_m}{2} \sqrt{\frac{L_{lk}}{C_{sn}}} \tag{5}$$

where  $I_m$  is the magnetizing current. Combining the previous equations, it is straightforward to derive the following expressions:

$$v_{Csn(max)} = V_g \frac{N_r}{N_p} + \frac{I_m}{2} \sqrt{\frac{L_{lk}}{C_{sn}}} \tag{6}$$

$$\Delta V_{Csn} = v_{Csn(max)} - v_{Csn(min)} = I_m \sqrt{\frac{L_{lk}}{C_{sn}}} \tag{7}$$

Figure 3 shows typical waveforms of a quasi-resonant flyback converter with an energy-regenerative snubber.

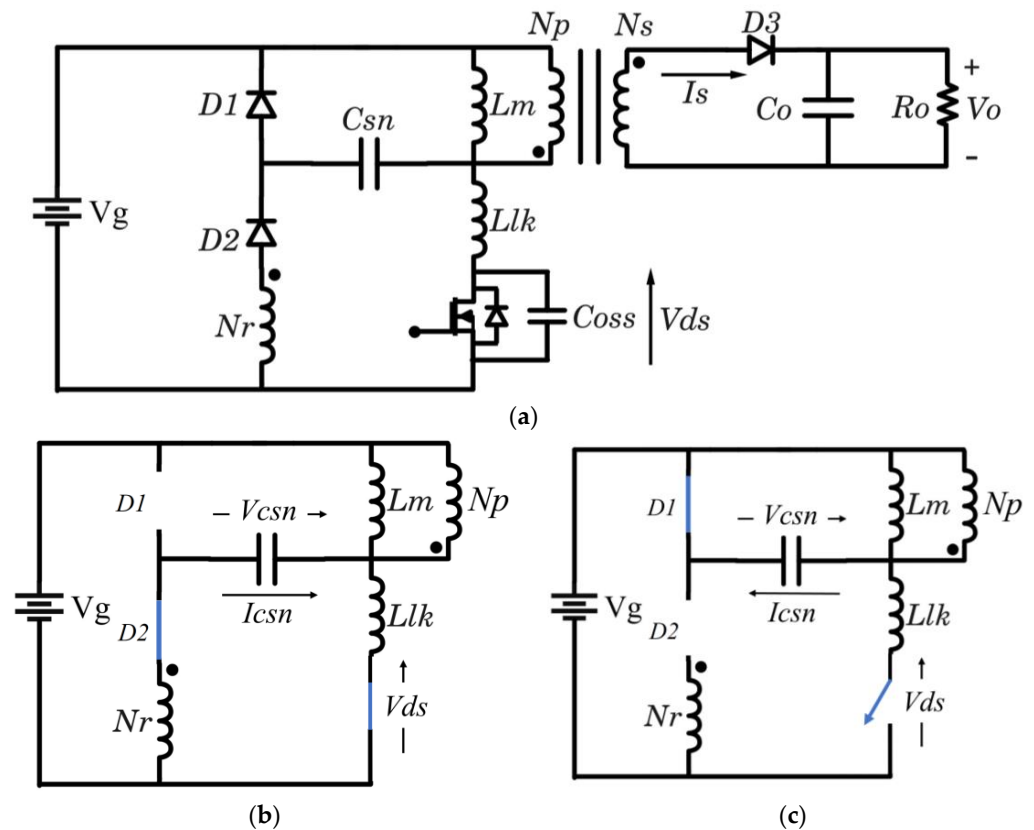


**Figure 2.** Flyback topology with regenerative snubber (a) Overall circuit (b) Snubber behavior during the on period (c) Snubber behavior during the off period.

During the switching, part of the energy not transferred to the secondary side is returned to the main.

The auxiliary winding turns ( $N_r$ ) and the snubber capacitance must be suitably sized depending on the characteristics of the converter.

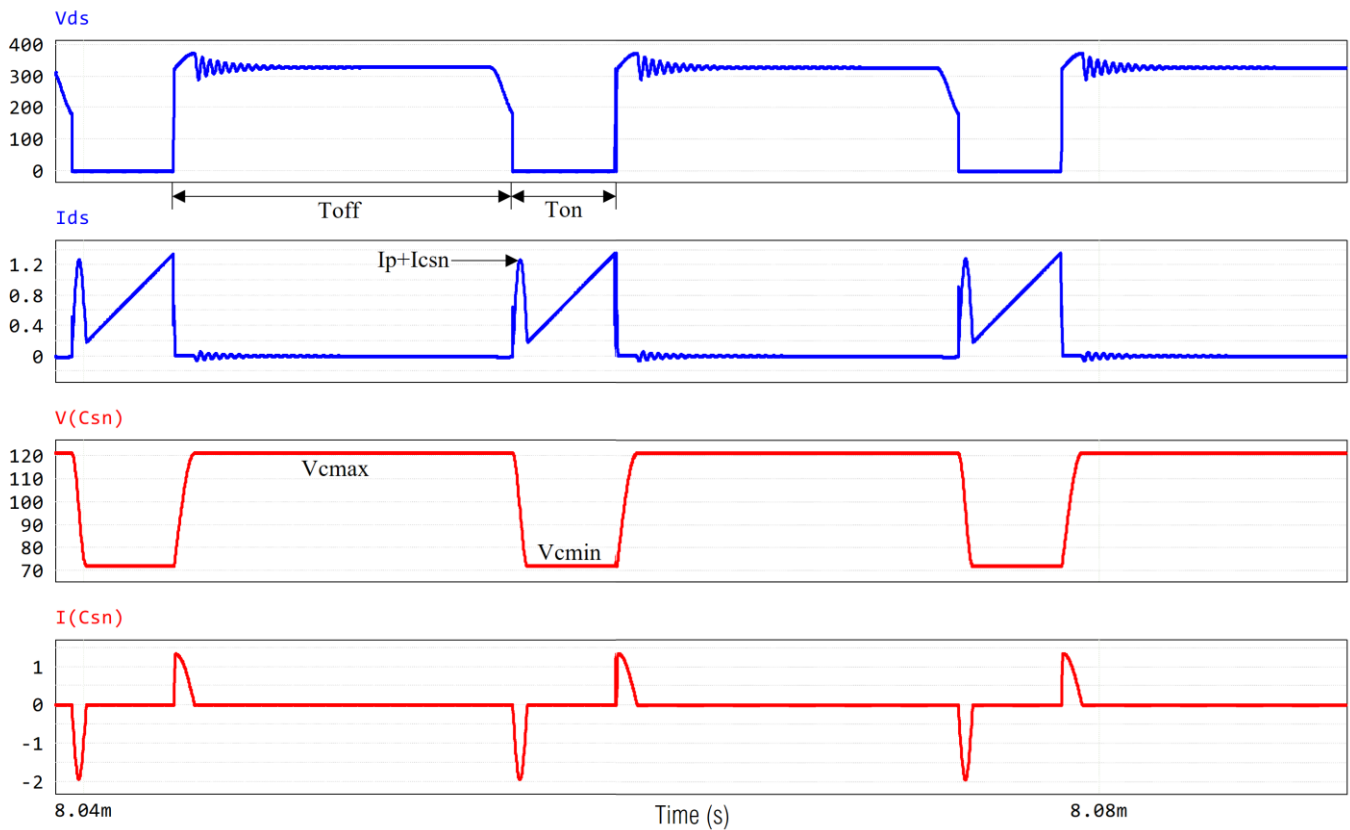


**Figure 3.** Typical waveforms of energy regenerative snubbers [21].

The selection of the maximum snubber capacitance is critical since the energy stored in the snubber is discharged into the power switch during its turn-on, thus causing a capacitive current spike whose amplitude and duration depend on the capacitance itself.

At the end of the leading-edge blanking, if the converter adopts a peak current mode control and the capacitive spike exceeds the current limitation imposed by the control loop time then the turn-on switching cycles might be prematurely stopped.

Additionally, the current flowing in  $D1$  and  $D2$  and the snubber capacitance current injected on the GaN channel at turn-on (which increases the RMS drain current) introduces extra conduction losses which must be evaluated to appropriately design the regenerative snubber.

The working principle described above may change when the input voltage is reduced enough to keep in conduction both diodes.

This would prevent the snubber capacitance from being fully charged during the switch off-state as both diodes would be forward-biased by the voltage levels imposed by the circuit. This must be considered during the design phase of the regenerative snubber, as the input voltage varies over a wide range.

### 3. Converter Design and Simulation

This study aims to design a regenerative snubber for a GaN-based 65 W Quasi-Resonant Flyback USB-PD converter that can achieve efficiency higher than an RCD snubber solution. To analyze and design the regenerative snubber for a wide range of input voltage and variable output voltage, the converter was modeled and simulated using PSIM software (version 2021b). This allowed us to analyze the main differences under various operative conditions.

To properly characterize a power supply with variable input and output voltages, it was necessary to impose worst-case conditions at the output (20 V/3.25 A). Figure 4 shows the simulated circuit in PSIM together with the diode and transformer main quantities,

while Table 1 reports other related quantities. In the considered model, only the components involved in the clamping process are modelled with any reasonable parasitic effects. The GaN device was modeled considering an ideal power switch with a series resistance to consider the device  $R_{DS-ON}$  and a parallel capacitance  $C_{OSS}$  (it is equal to a capacitor with a constant capacitance that would give the same stored energy as  $C_{OSS}$  while  $V_{DS}$  is rising from 0 V to 400 V). The device's main electrical characteristics are reported in Table 2. The remaining components are simulated using their ideal models. In this way, only the loss contribution due to the regenerative snubber (diodes, capacitance, and auxiliary windings) and the power switch affect the overall efficiency.

**Table 1.** Main quantities in the simulation model.

| Quantity  | Value        |
|-----------|--------------|
| $V_O$     | 20 V         |
| $P_{out}$ | 65 W         |
| $V_R$     | 133.3 V      |
| $C_{in}$  | 120 $\mu$ F  |
| $C_o$     | 1.36 mF      |
| ESR       | 5 m $\Omega$ |

**Table 2.** Electric characteristics of the GaN switch (Typical values at  $T_J = 25^\circ\text{C}$ ,  $V_{GS} = 6\text{ V}$ ).

| Parameter                     | Symbol              | Value                   |
|-------------------------------|---------------------|-------------------------|
| DC blocking voltage           | $V_{BL(DSS)}$       | 650 V                   |
| Drain transient voltage       | $V_{DS(transient)}$ | 750 V                   |
| Drain-to-source On resistance | $R_{DS-ON}$         | 225 m $\Omega$ (@2.2 A) |
| Equivalent output capacitance | $C_{OSS}$           | 22 pF                   |
| Total gate charge             | $Q_G$               | 1.5 nC                  |

The waveforms reported in Figure 5 were obtained by simulating the converter with a constant input voltage ( $V_g = 400\text{ Vdc}$ ). As shown in the figure, before the turn-off, the voltage across the snubber capacitance,  $V_{C_{sn}}$ , is equal to  $V_{C_{min}}$ . At turn-off, the diode  $D1$  is forward-biased due to the leakage energy, and the voltage at the anode of  $D1$ , i.e.,  $V_x$ , will be almost equal to the input voltage  $V_g$ . At the same instant, due to the bootstrap effect of the snubber capacitance, the voltage at the drain node,  $V_{ds}$ , must be equal to  $V_g + V_{C_{min}}$ .

To transfer the energy from the primary to the secondary, the diode  $D3$  must be forward-biased, which means that the drain voltage must be higher than  $V_g + V_R$ , where  $V_R$  is the reflected voltage, i.e., the output voltage reported to the primary winding through the primary to secondary turn ratio ( $N_p/N_s$ ).

If  $V_{C_{min}} < V_R$ , the energy transfer will be delayed with respect to the turn-off instant. This delay depends on the increasing of the drain voltage up to  $V_g + V_R$ , due to the energy leakage inductance. This consideration allows us to estimate the minimum value of the snubber capacitance.

The energy associated with the leakage inductance can be expressed as:

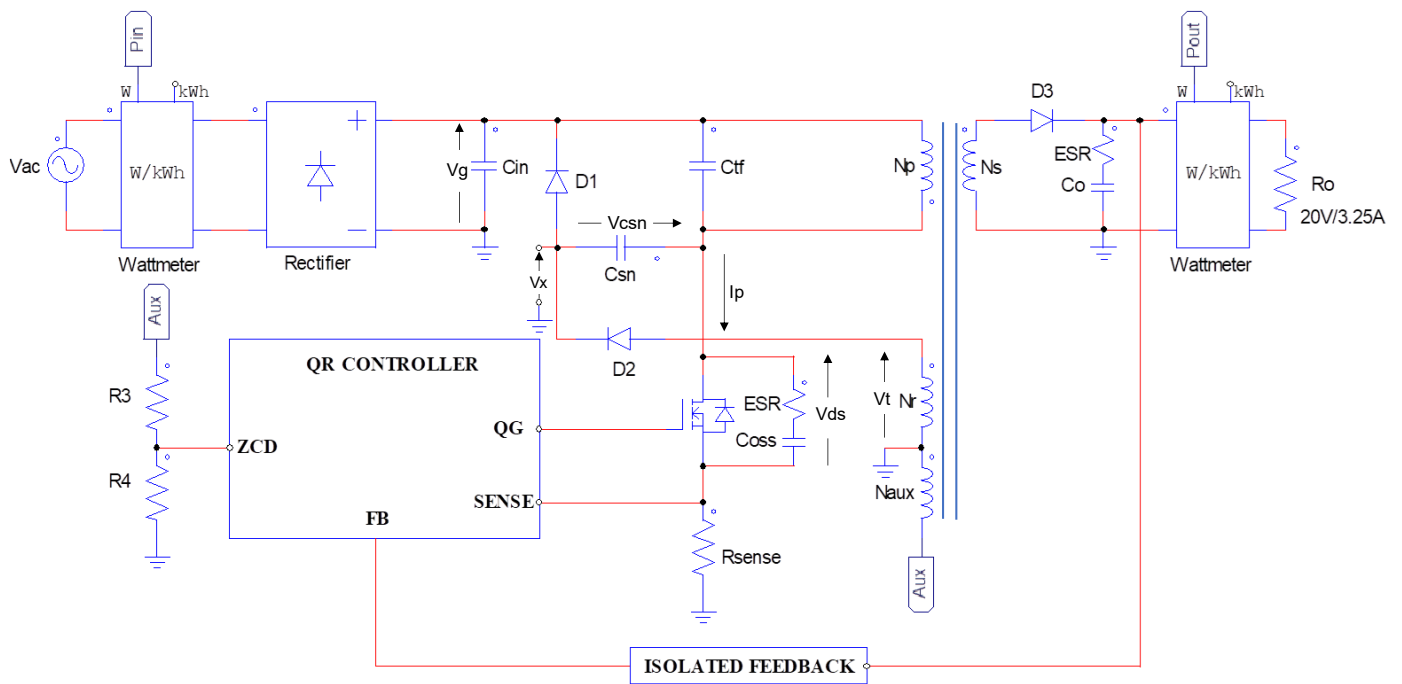
$$E_{lk} = \frac{1}{2} L_{lk} (I_{pk})^2 \quad (8)$$

where  $I_{pk}$  is the drain current at the end of the on time.

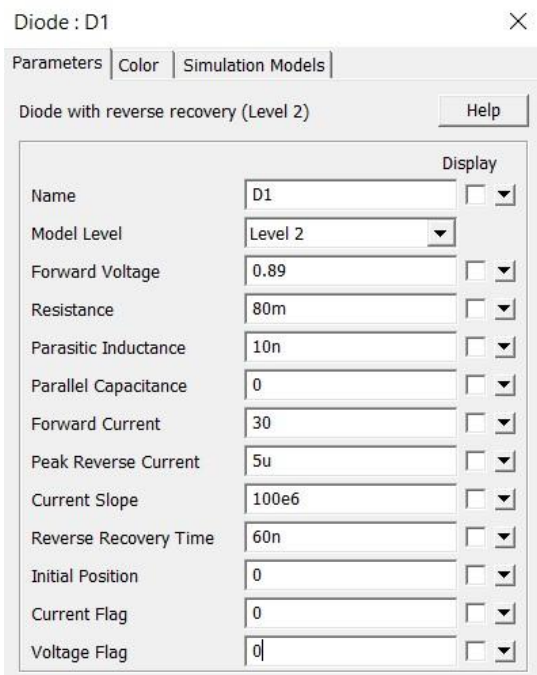
The same amount of energy will charge the snubber capacitance from  $V_{C_{min}}$  to  $V_{C_{max}}$ , then it can be also expressed as

$$E_{C_{sn}} = \frac{1}{2} C_{sn} (\Delta V)^2, \quad (9)$$

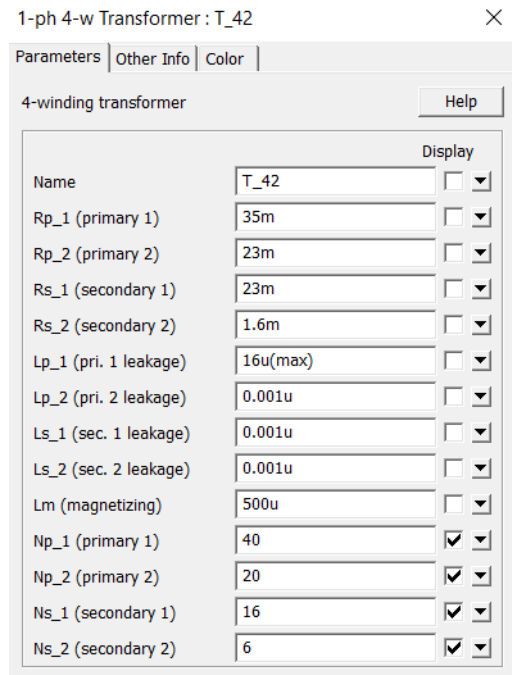
where  $\Delta V$  is the difference between the voltage drops  $V_{C_{max}}$  and  $V_{C_{min}}$ .



(a)



(b)



(c)

**Figure 4.** PSIM Model and main quantities of the considered Quasi-Resonant GaN-based Flyback Converter with Regenerative Snubber (a) Circuit model (b) Quantities of the snubber diodes (c) Quantities of the transformer.

Combining Equation (8) with (9) is possible to get the snubber capacitance as:

$$C_{sn} = \left( \frac{I_{pk}}{\Delta V} \right)^2 L_{lk} \quad (10)$$



Moreover, the peak value of the voltage at the drain node can be expressed as:

$$V_{ds,peak} = V_g + V_R + \Delta V. \quad (11)$$

The maximum allowed drain voltage is defined by the AMR of the device from which also derives the minimum value of the snubber capacitance which can be exploited in the regenerative snubber:

$$C_{snmin} = \left( \frac{I_{pk}}{\Delta V_{max}} \right)^2 L_{lk}, \quad (12)$$

where:

$$\Delta V_{max} = V_{dsmax} - V_{gmax} - V_R. \quad (13)$$

The power supply being analyzed has an input voltage of 90 Vac to 264 Vac.

Since the converter is designed for USB-PD applications, the output voltage is variable in a range between 5 V and 20 V. Therefore, the worst case, from the power switch standpoint, is with  $V_o = 20$  V and  $V_{in} = 264$  Vac, which results in the maximum voltage stress across the drain.

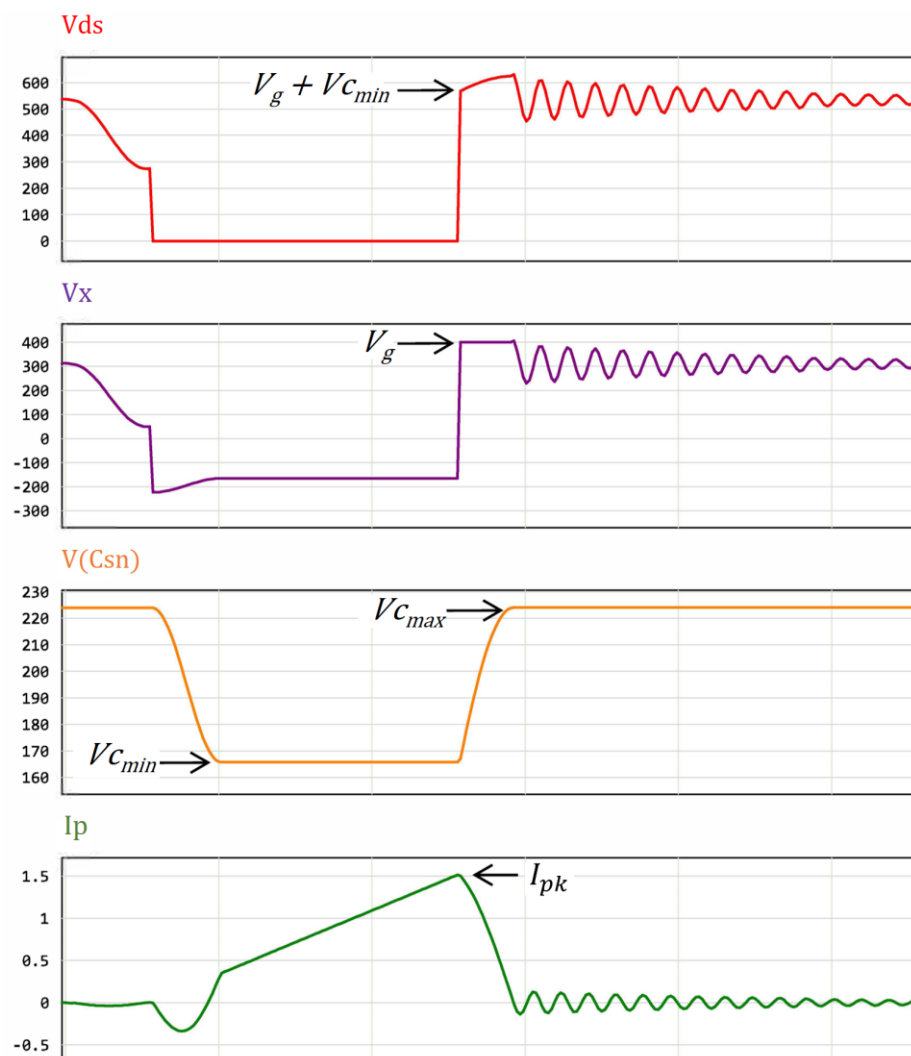
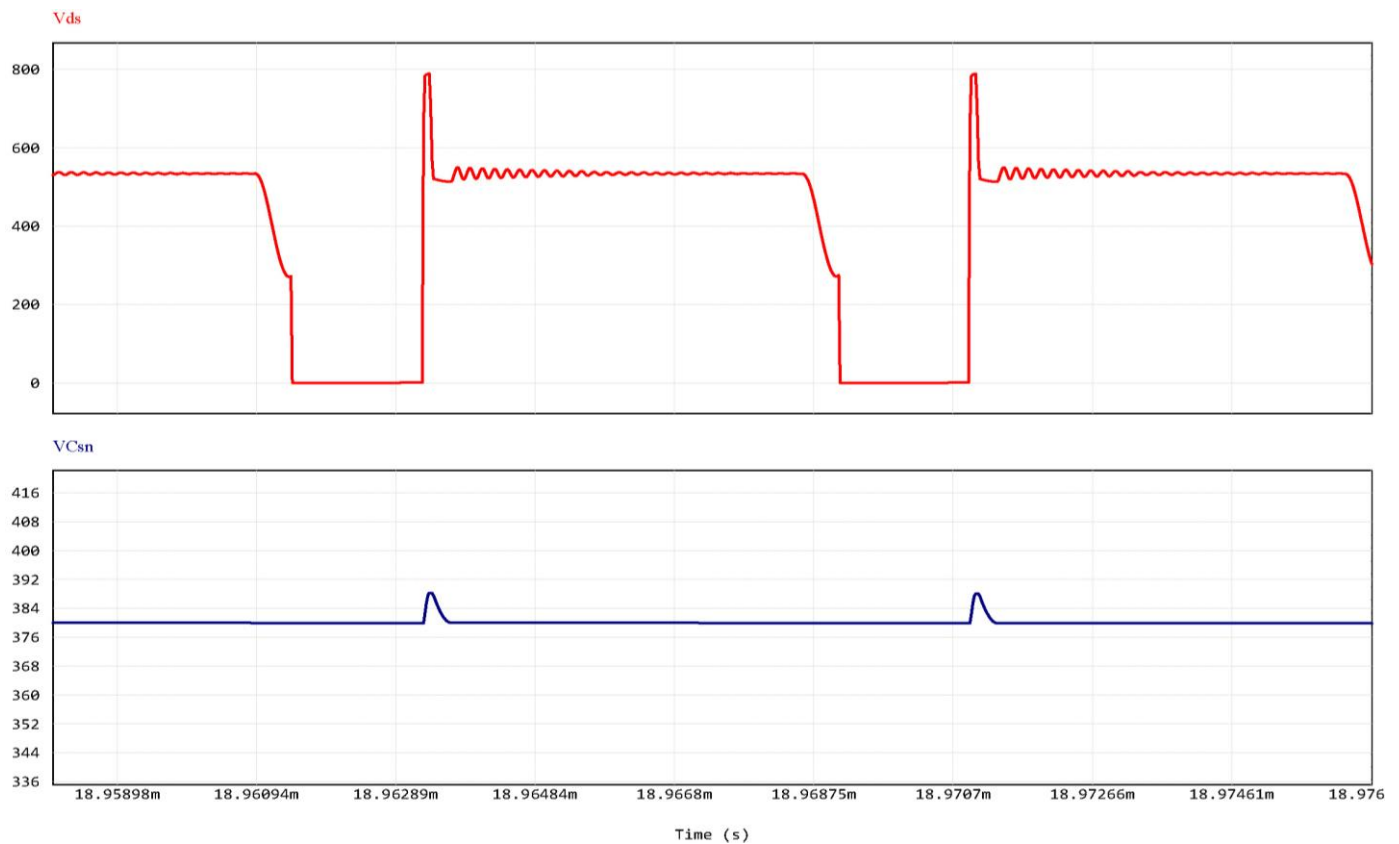


Figure 5. Flyback converter simulation with regenerative snubber main waveforms.

For simulation purposes, it is possible to define a maximum number of turns of the auxiliary winding  $N_r$ . As is shown in Figure 6, for a given value of the snubber capacitance, the snubber effect decreases rapidly as  $N_r$  approaches the number of turns

of the primary winding  $N_p$ . Consequently, the voltage variation affecting the snubber capacitance decreases, and the peak voltage at the drain node increases, reaching values that can exceed the device's AMR.



**Figure 6.**  $V_{ds}$  and  $V_{c_{sn}}$  for  $N_r = N_p$ .

When the converter is supplied with an input voltage of 115 Vac, the peak DC input voltage  $V_g$  is approximately equal to 150 Vdc. This implies that the operating principle of the regenerative snubber differs from what is described in Section 2.

Its specific mode of operation can be analyzed by examining the waveforms obtained in the simulation, which are shown in Figure 7.

As discussed in Section 2, the voltage across the snubber capacitance, before the turn-off, is equal to  $V_{c_{min}}$ . At turn-off, the leakage energy forces the current to flow through  $D1$ , which is forward-biased. Therefore, the voltage  $V_x$  can be considered almost equal to the input voltage  $V_g$ . Since the voltage across a capacitor cannot change instantaneously, the drain voltage increases up to  $V_g + V_{c_{min}}$ , due to the bootstrap effect. During this phase, the leakage energy is transferred to the snubber capacitor thus increasing the drain voltage. Once this energy is completely transferred, the diode  $D1$  will no longer be forward-biased and the  $V_x$  node becomes floating.

In this condition, the parasitic elements cause drain voltage oscillation and, due to the bootstrap effect, even the  $V_x$  node oscillates at the same frequency. The voltage  $V_t$ , at the anode of  $D2$ , is forced by the output voltage and the turn ratio windings: in the simulation of Figure 7, the worst-case condition is considered, i.e.,  $V_o = 20$  V.

If  $V_x$  decreases below  $V_t$ , due to the oscillations, the diode  $D2$  starts to conduct, and the snubber capacitor is slightly discharged. As long as  $D2$  is forward biased,  $V_x$  is equal to  $V_t$  minus the voltage drops across  $D2$ .

During this interval, part of the energy of the snubber capacitor is transferred to the secondary side.

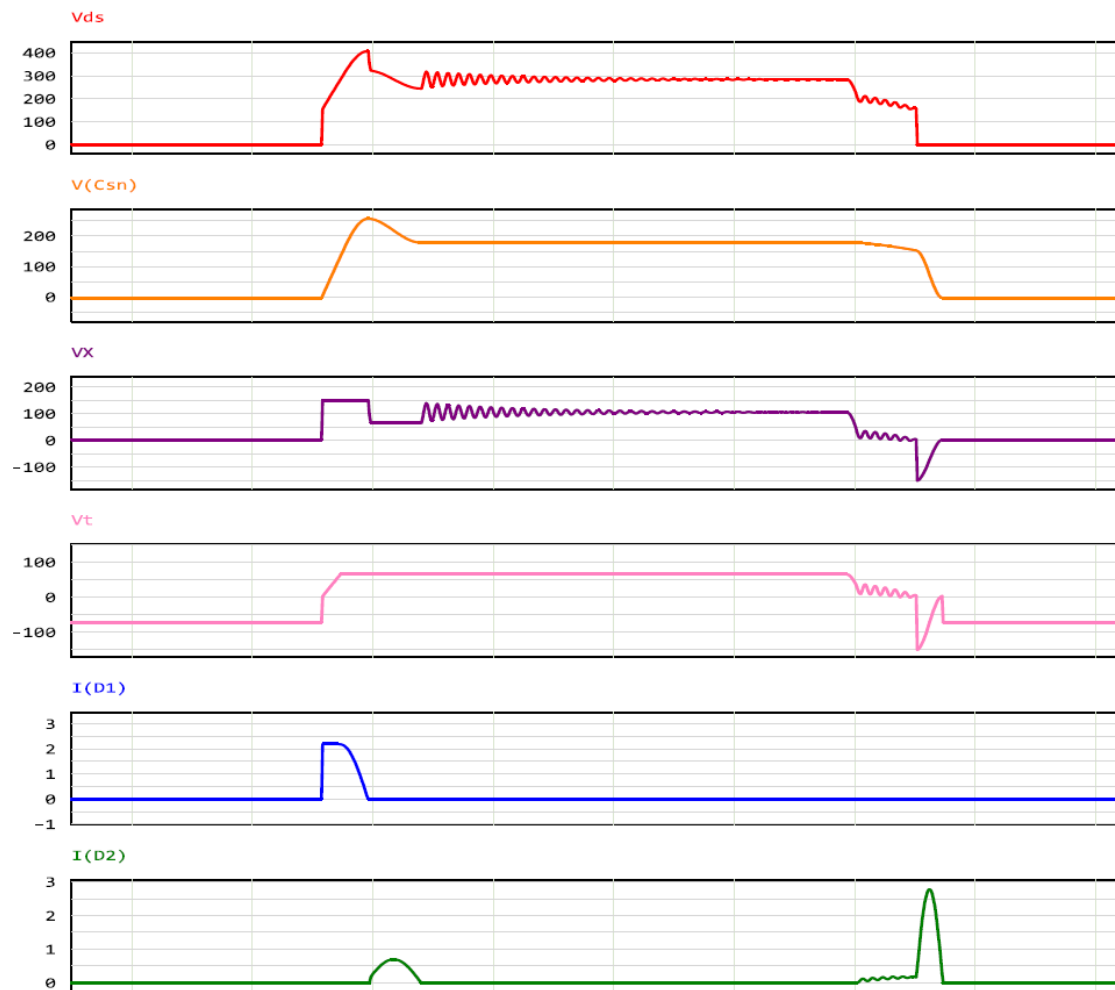


**Figure 7.** Flyback main waveforms for low input voltage.

$D2$  also conducts in another short interval during the off period, after the primary inductance demagnetization. In detail, once the primary inductance is completely demagnetized, the secondary diode  $D3$  will no longer be forward biased and, consequently, the anode of  $D2$  can be considered floating, due to the interaction with the anode of  $D3$  through the auxiliary to secondary turn ratio.

During this period, both  $D2$  terminals are floating, thus  $V_t$  and  $V_x$  follow the drain oscillations. Considering that  $V_x$  is equal to the drain voltage reduced by the auxiliary to primary turn ratio, then  $V_t$  decreases less than  $V_x$ , thus the  $D2$  diode becomes forward biased.

Once  $D2$  starts to conduct, a current flows through the GaN's output capacitance involving a slight charge that opposes its discharges after demagnetization. Due to this phenomenon, when the switch is turned-on, the  $V_{ds}$  will be higher than  $V_g - V_R$  (that is the nominal value of a QR mode flyback converter), thus increasing the switching losses.

It is worth noting that this phenomenon does not occur at higher input voltage, where  $D2$  is forward-biased at the turn-on only.

#### 4. Choice of the Optimum Parameters

The snubber efficiency in function of its capacitance and auxiliary winding number of turns has been evaluated by parametric simulations. The efficiency has been expressed as the ratio between the input energy and those delivered to the load. These quantities have been indirectly obtained using the two wattmeters, placed as shown in Figure 4.

In the considered model, only the components involved in the clamping process are modeled with any reasonable parasitic effect. The remaining components are simulated

using their ideal models. In this way, the loss contribution due to the regenerative snubber (diodes, capacitance, and auxiliary windings) and the power switch affect the efficiency. Therefore, the result of the parametric simulation is an exhaustive search that returns a qualitative curve useful to identify the optimal values of  $C_{sn}$  and  $N_r$  that maximize the efficiency without the need to use any specific optimization technique.

In the simulations,  $N_r$  was varied from 10 to 40 and, the snubber capacitance  $C_{sn}$  was varied from 1 nF and 10 nF, according to Equation (12), the other quantities are set to the values reported in Figure 4b,c and Tables 1 and 2. In such a case, being discrete and limited the search space due to component admissible values, as mentioned before, it was not necessary to adopt any optimization technique, which is usually used when one needs an optimal design with a limited number of evaluations of the objective function.

The first parametric simulation enabled us to understand the influence of the auxiliary winding number of turns on the drain voltage. This allowed us to exclude the  $N_r$  values leading to a voltage higher than the selected  $V_{dsmax}$ . Figure 8 shows the results of this parametric simulation.

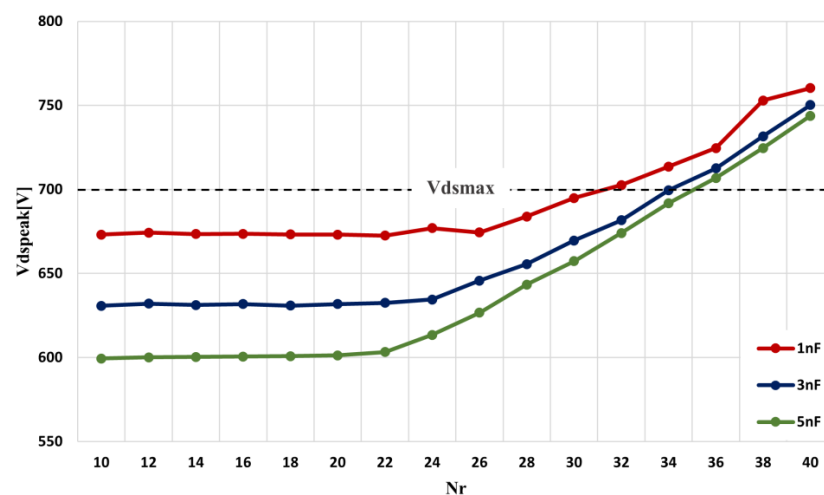


Figure 8. Max  $V_{ds}$  vs.  $N_r$ .

As explained in the previous section and as shown in Figure 8, the snubber effect decreases when  $N_r$  is greater than 20. Moreover, the parametric evaluation with  $N_r \geq 30$  is pointless, because the peak on the drain voltage exceeds the maximum acceptable value (700 V) in the worst case ( $C_{sn} = C_{snmin}$ ).

In the second step of the parametric simulation, the power supply was powered with an input voltage of 230 Vac while the output voltage was set to 20 V at maximum load. The snubber capacitance and number of turns were varied within their range. Figure 9 shows some curves that were obtained by processing the results returned by the parametric simulation. These curves indicate that the efficiency changes as the number of turns of the auxiliary winding varies for three different values of  $C_{sn}$ .

The efficiency curves have a maximum when  $N_r = 20$ , and then it decreases. When the converter operates at 115 Vac, the optimal value of the number of turns is lower than 20.

However, since the aim of the study is the optimization of the power density, the maximization of the efficiency at 230 Vac has been considered as the main target, being the snubber losses higher than at 115 Vac.

Although the curves in Figure 9 indicate a slight increase in the efficiency as the snubber capacitance increases, another set of simulations was performed to exactly determine the optimum value of the snubber capacitance,  $C_{sn}$ . The converter efficiency and the snubber diode losses were evaluated by varying the snubber capacitance in a range between 500 pF and 10 nF, maintaining a constant number of turns ( $N_r = 20$ ). Capacitances lower than  $C_{min}$ , i.e., 1 nF, are only used to draw the qualitative efficiency curve, because, for this value,  $V_{ds}$  exceeds the AMR voltage. Simultaneously, the snubber capacitance cannot

be greater than 3 nF, because of the high extra current that would occur on the device at turn-on, as is already discussed, causing a premature termination of the conduction cycle of the power GaN.

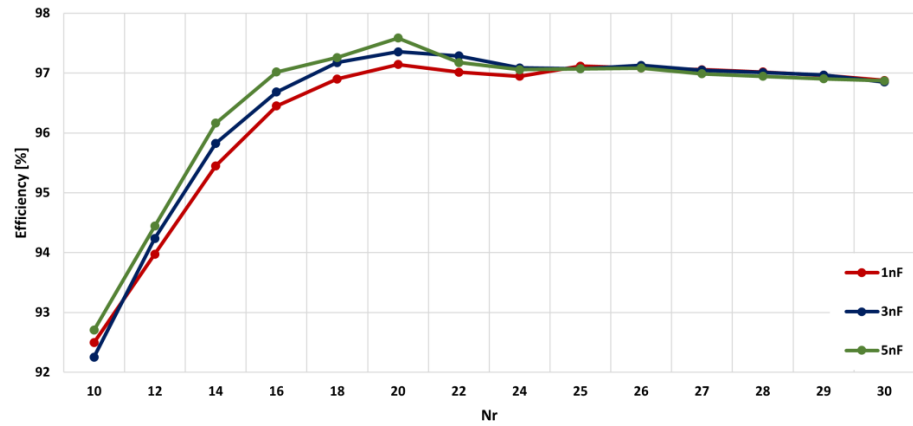


Figure 9. Efficiency vs.  $Nr$  for different values of the snubber capacitance at 230 Vac.

Further parametric simulations have been performed under low input voltage (150 Vdc) and output load equal to 25% (0.81 A) conditions. At low input voltage, the diode losses increase with increasing the snubber capacitance. Moreover, these contributions are not negligible compared to the switching losses. Additionally, the low output load involves low GaN conduction losses, making significant the diodes losses.

For all these reasons, under the selected simulation conditions, an increase in the snubber capacitance involves an increase in the diode losses and, consequently, a significant efficiency reduction. Figure 10 show the snubber efficiency and power dissipated by diodes D1 and D2 as the snubber capacitance varies.

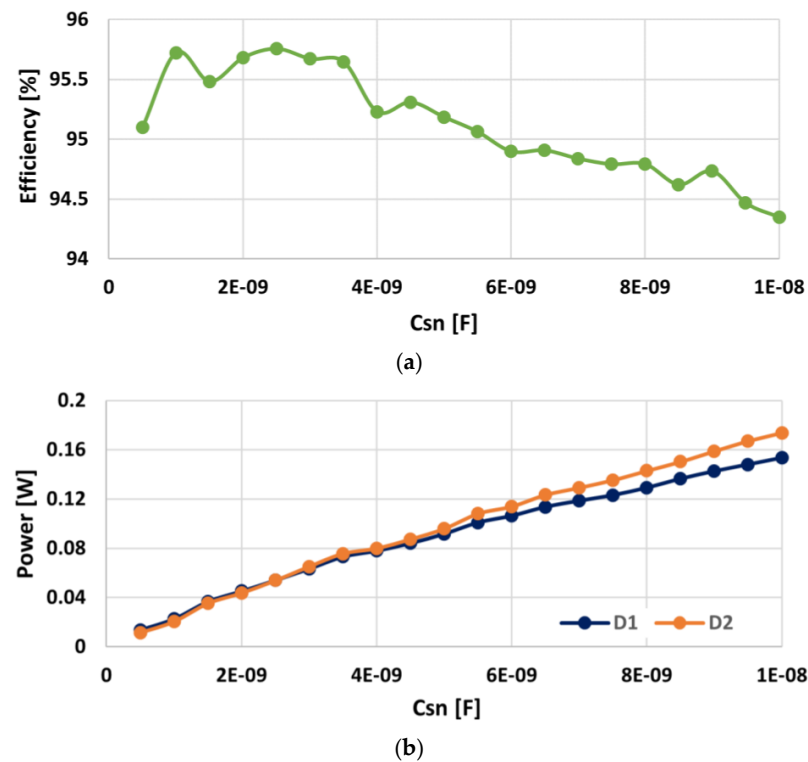


Figure 10. (a) Efficiency Curve for high input voltage and low load. (b) Diodes Power Consumption for high input voltage for low load.

Moreover, the one just reported represents the most interesting result since in the case of high input voltage and low input voltage at maximum load conditions, an increase in snubber capacitance led to a very slight increase in efficiency. Considering both cases, it can be deduced that the optimal snubber capacitance is the minimum value (1 nF).

## 5. Experimental Results

An STMicroelectronics evaluation board of a 65 W USB-PD isolated power supply has been used to test the proposed solution. The board is designed for a wide range input voltage range, i.e., 90 to 264 Vac, with 4 fixed output dc profiles: 5 V@3 A; 9 V@3 A; 15 V@3 A; 20 V@3.25 A.

The evaluation board implements a quasi-resonant flyback converter based on the VIPERGAN65, a High Voltage (HV) converter with optocoupler feedback for voltage regulation. This controller combines a high-performance low-voltage Pulse Width Modulation (PWM) controller chip with a 650 V E-Mode GaN HEMT (Gallium Nitride High Electron Mobility Transistor) power switch integrated in the same package. The main electrical parameters of the GaN power switch are reported in Table 2.

Figure 11 represents the top and the bottom sides of the application board. In the bottom side of the board, it is possible to identify the RCD snubber characterized by the diode D1, the capacitance C4 and the resistances R3, R4, R5, and R18, which is better shown in Figure 12.

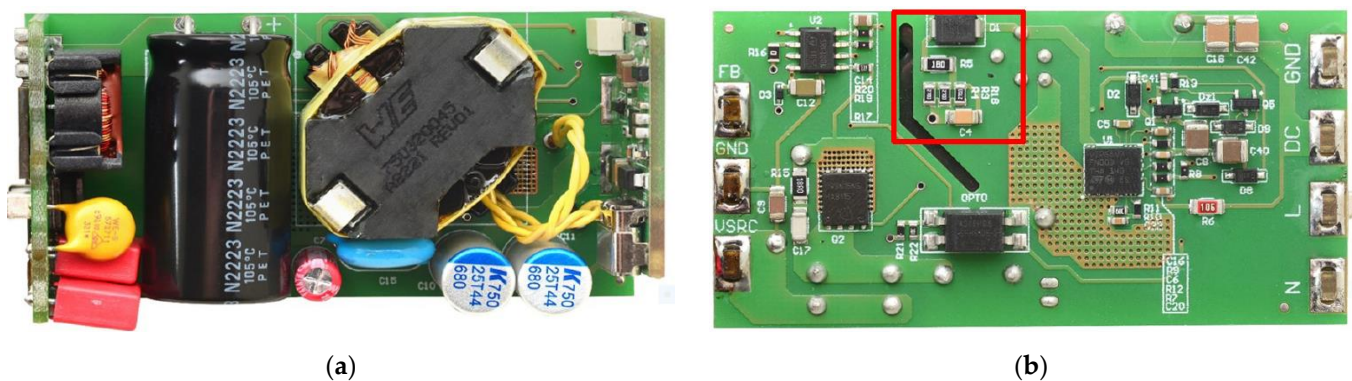


Figure 11. Application board: (a) top view; (b) bottom view. A magnification of the red box is reported in Figure 12.

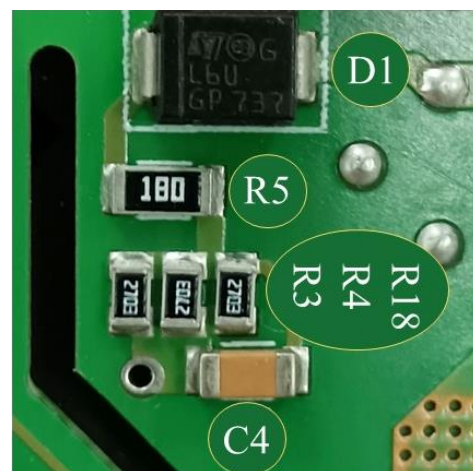


Figure 12. RCD Snubber components.

Therefore, the evaluation board has been appropriately modified. In detail, according to the outcome of the simulation results, the transformer was replaced with a new one,

characterized by an additional auxiliary winding with  $Nr = 20$ . The RCD snubber was removed from the board and replaced with the designed regenerative solution.

The goal of the experimental phase was the comparison of the RCD clamp and regenerative snubber solutions. To this aim, the efficiency curves of the offline converter with varying input voltage, output voltage and load have been obtained by measurements.

Part of the experimental setup is reported in Figure 13 which was characterized by:

- 2 Digital Power Meter (Yokogawa, Belgrade, Serbia, WT310E)
- DC Electronic Load (Chrom, Pune, India, 63,105–1 A/10 A–125 V/500 V–300 W)
- AC Power Source/Analyzer (Agilent, Santa Clara, CA, USA, 6812 B–300 Vrms–750 VA)
- Mixed Signal Oscilloscope (Tektronix, Beaverton, OR, USA, MSO54B)
- High Voltage Probes (Tektronix P5100A–500 Mhz–40 M $\Omega$ –2.5 pF–1000 V CAT2)
- Current Probes (Tektronix TCP0030A–120 Mhz–5 A/30 A–300 V CAT2)
- Power-Z USB Tester (ChargerLAB, Monterey Park, CA, USA, KM003C)

The main waveforms were analyzed by supplying the application board at the nominal input voltages of 115 Vac and 230 Vac, to verify that the regenerative snubber perform as predicted in simulation. Figures 14 and 15 show the main experimental and simulated waveforms at 230 Vac and 115 Vac, respectively.

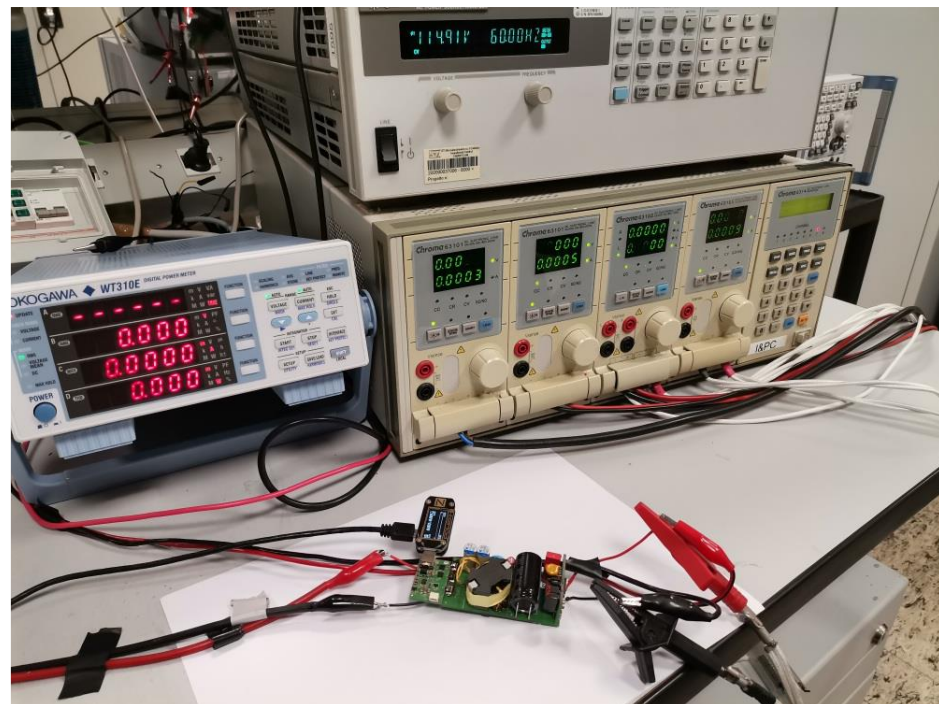


Figure 13. Measurement Setup and Application Board.

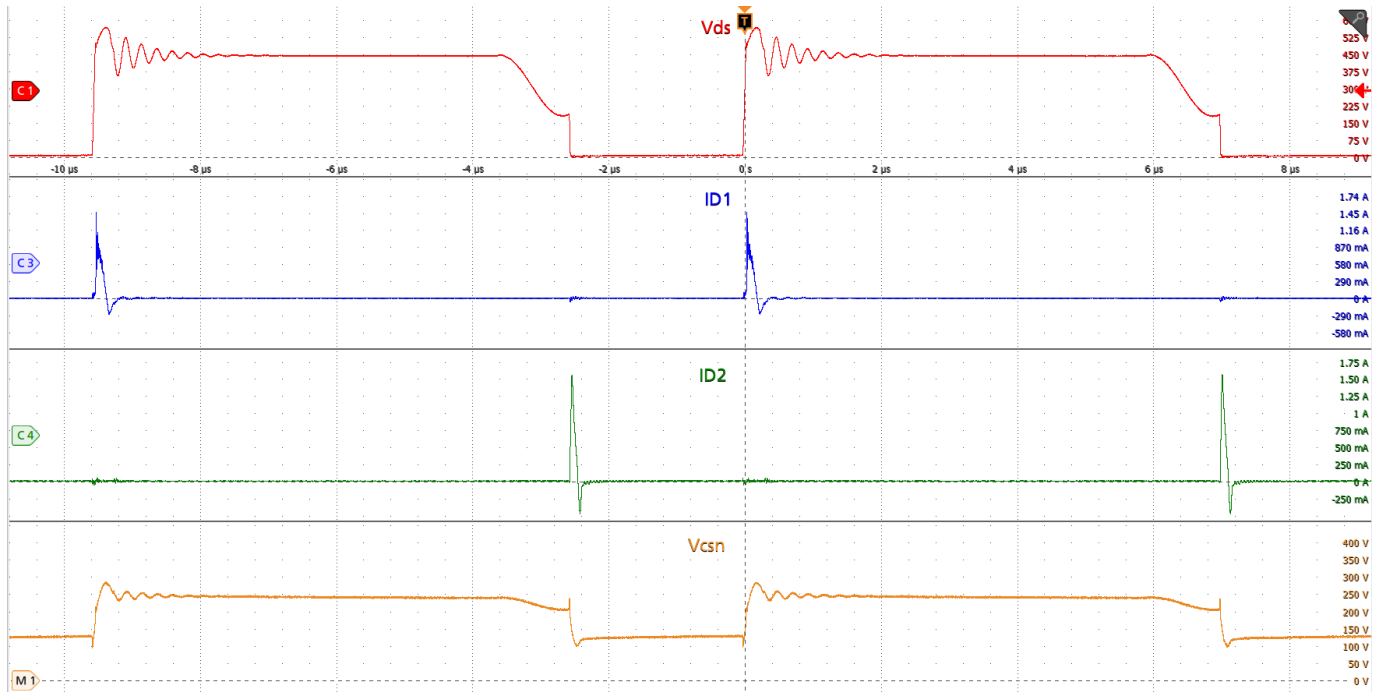
Tables 3 and 4 report a comparison between PSIM simulation and experimental results.

Table 3. Parameters Comparison at 230 Vac.

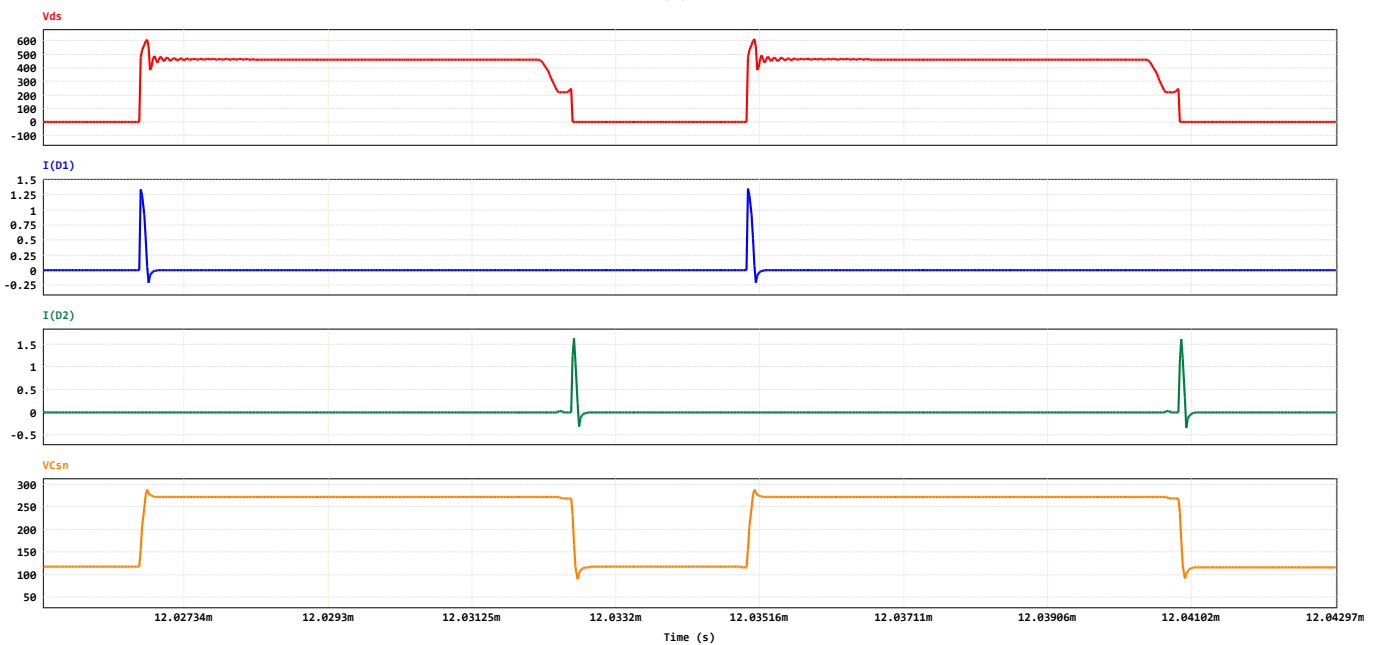
| Parameter              | Simulation | Experimental |
|------------------------|------------|--------------|
| V <sub>ds</sub> (peak) | 576 V      | 562 V        |
| ID1 (peak)             | 1.32 A     | 1.45 A       |
| ID2 (peak)             | 1.42 A     | 1.59 A       |
| V <sub>cmin</sub>      | 127 V      | 130 V        |
| V <sub>cmax</sub>      | 248 V      | 250 V        |
| f <sub>sw</sub>        | 118 KHz    | 109 KHz      |

**Table 4.** Parameters Comparison at 115 Vac.

| Parameter  | Simulation | Experimental |
|------------|------------|--------------|
| Vds (peak) | 471 V      | 476 V        |
| ID1 (peak) | 2 A        | 1.92 A       |
| ID2 (peak) | 0.6 A      | 0.7 A        |
| Vcmin      | 67 V       | 75 V         |
| Vcmax      | 196 V      | 200 V        |
| fsw        | 67 KHz     | 65 KHz       |



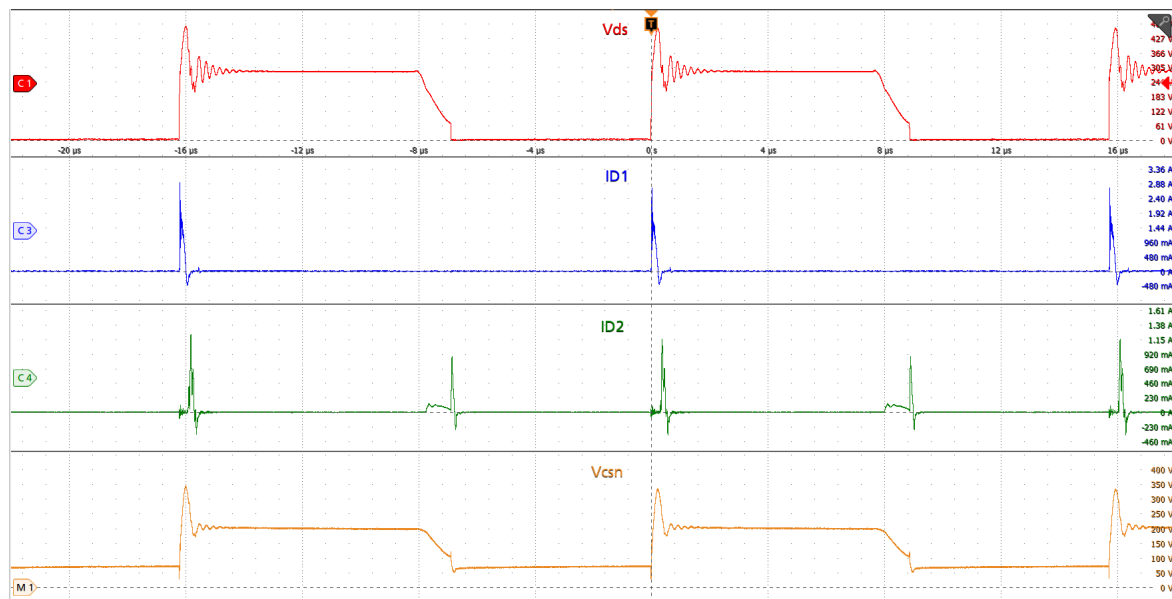
(a)



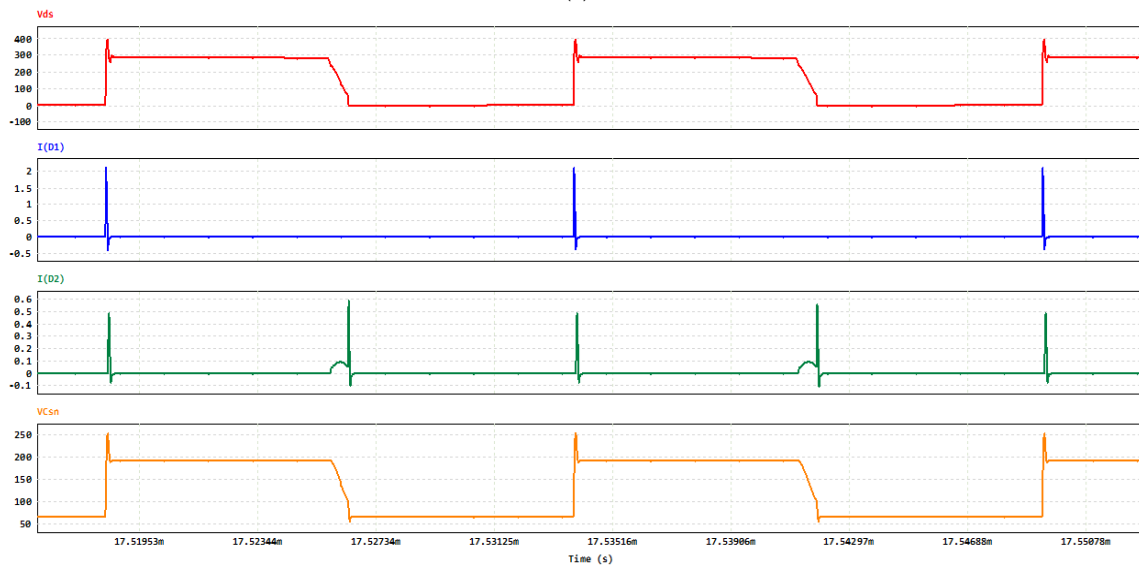
(b)

**Figure 14.** Main waveforms at 230 Vac input voltage: (a) Experimental results (b) PSIM Simulation.





(a)



(b)

**Figure 15.** Main waveforms at 115 Vac input voltage: (a) Experimental results (b) PSIM Simulation.

The experimental results show that the circuit model used in the simulation accurately emulates the behavior of the application board.

To obtain comparable efficiency measurements with the two snubber configurations, it is necessary to have the same snubber effect, i.e., similar peak drain voltage under similar operating conditions. For this reason, the drain node voltage was evaluated in the worst operating conditions: maximum input voltage (264 Vac), maximum output voltage (20 V) and load conditions (3.25 A). This approach allows us to verify if the regenerative snubber component values give a sufficient snubber effect while maintaining the peak drain voltage always lower than the device AMR (in Figure 16,  $V_{dsmax}$  is approximately equal to 638 V).

This demonstrates that the optimum capacitance (1 nF), causes a peak on the drain node lower than the AMR. To achieve the same snubber effect (similar  $V_{dsmax}$ ), when RCD snubber is used, the snubber capacitance is maintained at 1 nF while it must be chosen an appropriate snubber resistance value. Moreover, the same transformer is used to maintain the same leakage inductance for both measurements.

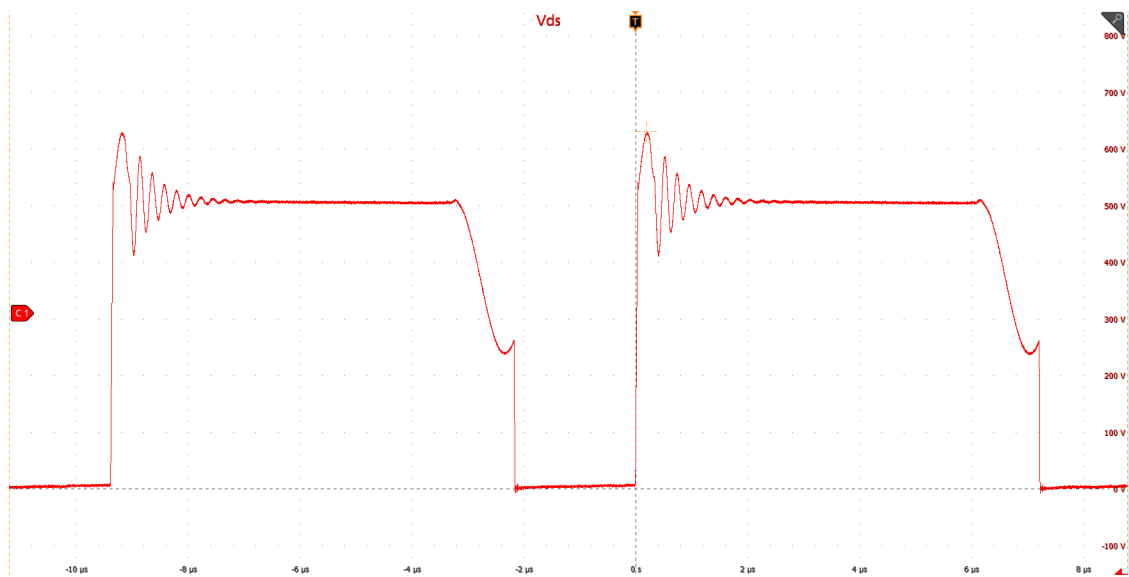


**Figure 16.** Voltage at the drain node for 264 Vac input voltage.

The efficiency measurements have been performed at nominal input voltages (115 Vac and 230 Vac), for all output voltage profiles (5 V, 9 V, 15 V and 20 V).

The efficiency measurements have been performed by replacing the energy regenerative snubber with an RCD snubber maintaining the same snubber capacitance value to have the same snubber effect. The efficiency curves at different operative conditions are compared and reported in Figures 17 and 18. The plots show that the efficiency in the case of regenerative solution is higher in both cases (low and high input voltage) regardless of the dc output profiles.

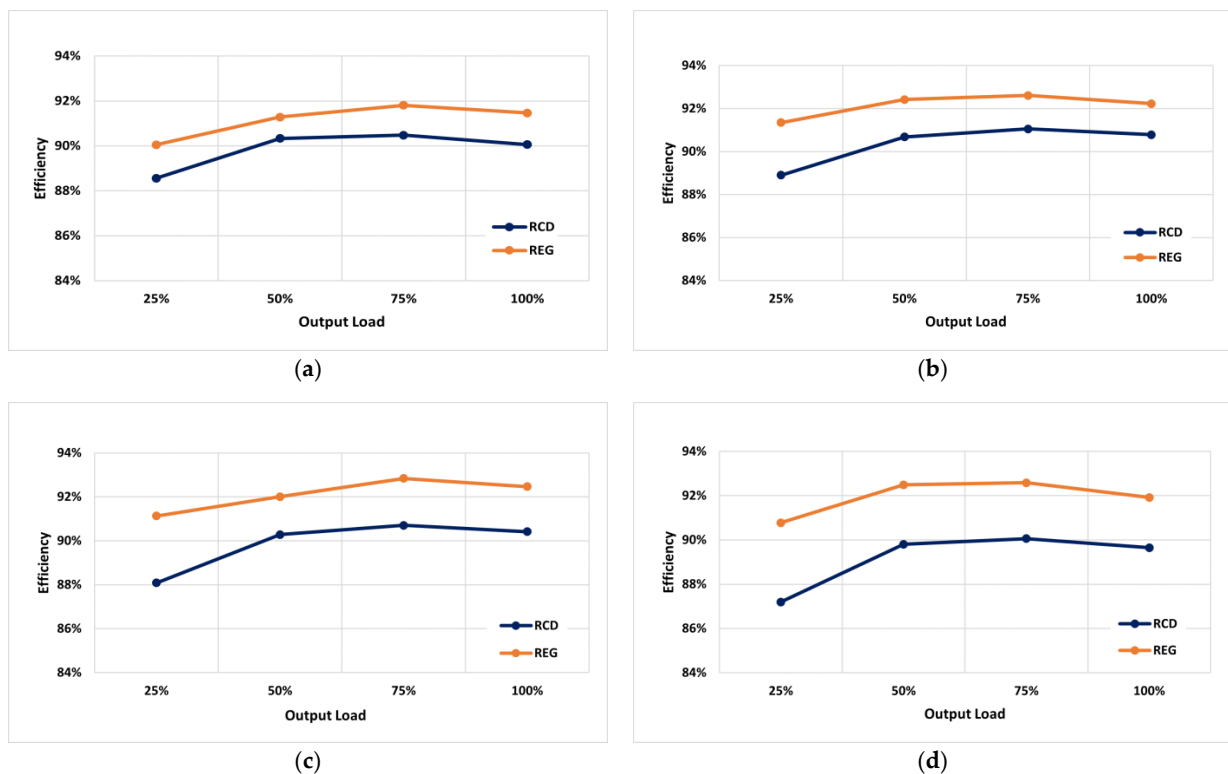


**Figure 17.** Efficiency Curves comparison for 115 Vac input voltage and output voltage equal to (a) 5 V, (b) 9 V, (c) 15 V, (d) 20 V.

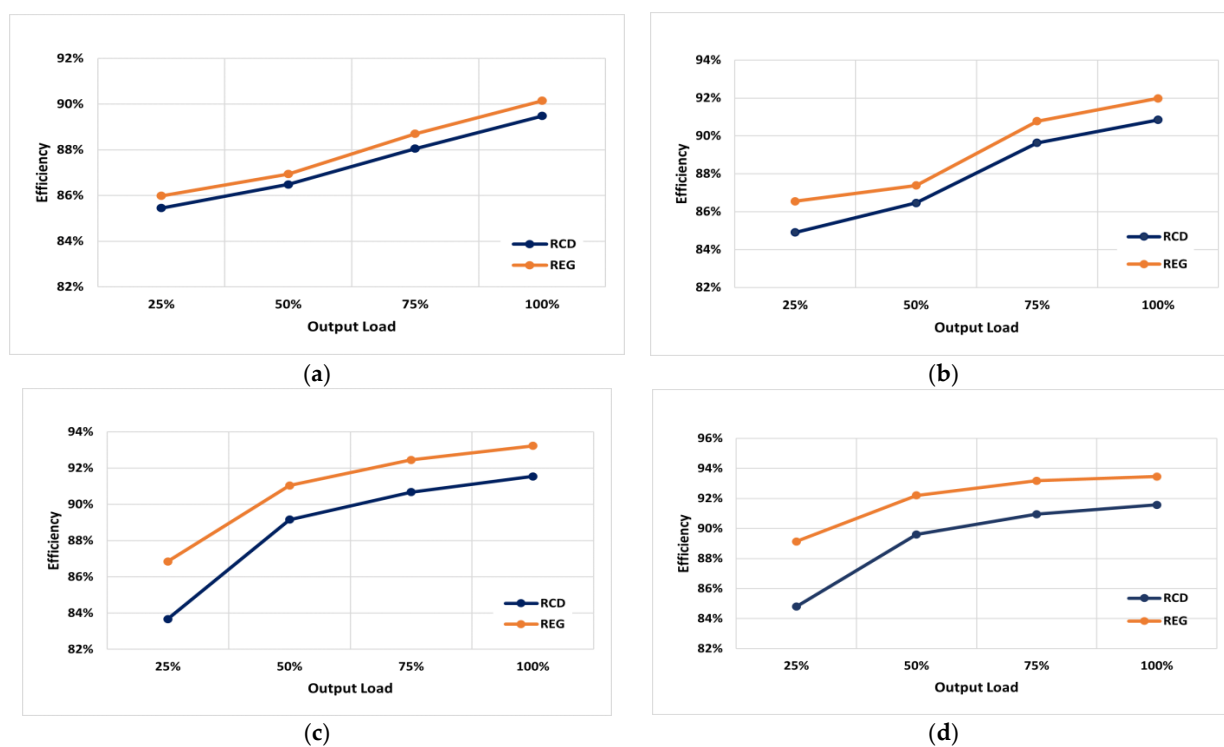


**Figure 18.** Efficiency curves comparison for 230 Vac input voltage and output voltage equal to (a) 5 V, (b) 9 V, (c) 15 V, (d) 20 V.

## 6. Conclusions

This work proposes an energy regenerative snubber for to improve the efficiency and power density in a GaN-based 65 W USB-PD Flyback Converter. Through the circuit modelling of the converter the behavior of the quasi-resonant converter has been analyzed. The simulations have predicted that the regenerative solution strongly reduces the drain voltage spike at the turn-off of the GaN device, because the energy associated with the leakage inductance is partially recovered, thus increasing the overall efficiency.

A set of parametric simulations has been executed to correctly design the regenerative snubber circuitry. Special attention was given to the sizing of the transformer's extra auxiliary winding and the snubber capacitor. These parametric simulations allowed us to obtain the optimal parameters from an efficiency point of view. A comparison in terms of overall efficiency between the proposed solution and standard RCD snubbers has been experimentally performed. From the bench analysis, it is possible to confirm that the regenerative snubber solution improves the efficiency compared to the RCD solution for each output fixed profile of the USB-PD converter and it is useful even for wide-range input voltage applications, so it can allow us to reach very high efficiency and power density.

**Author Contributions:** Writing—review and editing F.C., A.C., E.C. and S.A.R. All authors have read and agreed to the published version of the manuscript.

**Funding:** This research received no external funding.

**Data Availability Statement:** The data are available and explained in this article, and the readers can access the data supporting the conclusions of this study.

**Conflicts of Interest:** Author Fabio Cacciotto, Alessandro Cannone, and Emanuele Cassarà were employed by the company ST Microelectronics Co., Ltd. The remaining author declares that the research was conducted in the absence of any commercial or financial relationships that could be construed as a potential conflict of interest.

## References

1. Hwu, K.-I.; Shieh, J.-J.; Lin, C.-T. Universal Input Single-Stage High-Power-Factor LED Driver with Active Low-Frequency Current Ripple Suppressed. *Energies* **2024**, *17*, 183. [[CrossRef](#)]
2. Huang, A.B.-K.; Liang, B.T.-J.; Tseng, C.W.-J.; Chen, D.K.-H.; Chen, E.Q.-M. Primary-Side Control for Flyback Converter with Wide Range Operation. In Proceedings of the 2019 10th International Conference on Power Electronics and ECCE Asia (ICPE 2019—ECCE Asia), Busan, Republic of Korea, 27–31 May 2019; pp. 3108–3115. [[CrossRef](#)]
3. Quentin, N.; Perrin, R.; Martin, C.; Joubert, C.; Lacombe, B.; Buttay, C. GaN Active-Clamp Flyback Converter with Resonant Operation Over a Wide Input Voltage Range. In Proceedings of the PCIM Europe 2016; International Exhibition and Conference for Power Electronics, Intelligent Motion, Renewable Energy and Energy Management, Nuremberg, Germany, 10–12 May 2016; pp. 1–8.
4. Rizzoli, G.; Zarri, L.; Wang, J.; Shen, Z.; Burgos, R.; Boroyevich, D. Design of a two-switch flyback power supply using 1.7 kV SiC devices for ultra-wide input-voltage range applications. In Proceedings of the 2016 IEEE Energy Conversion Congress and Exposition (ECCE), Milwaukee, WI, USA, 18–22 September 2016; pp. 1–5. [[CrossRef](#)]
5. Lodh, T.; Majumder, T. A high gain highly efficient and compact flyback converter with a passive clamp circuit. In Proceedings of the 2016 International Conference on Signal Processing Communication, Power and Embedded System (SCOPEs), Paralakhemundi, India, 3–5 October 2016; pp. 1489–1494. [[CrossRef](#)]
6. Mohammadi, M.; Adib, E.; Farzanehfard, H. Passive lossless snubber for double-ended flyback converter. *IET Power Electron.* **2015**, *8*, 56–62. [[CrossRef](#)]
7. Pesce, C.; Riedemann, J.; Pena, R.; Jara, W.; Maury, C.; Villalobos, R. A Modified Step-Up DC-DC Flyback Converter with Active Snubber for Improved Efficiency. *Energies* **2019**, *12*, 2066. [[CrossRef](#)]
8. Yau, Y.-T.; Hung, T.-L. A Flyback Converter With Novel Active Dissipative Snubber. *IEEE Access* **2022**, *10*, 108145–108158. [[CrossRef](#)]
9. Balbayev, G.; Nussibaliyeva, A.; Tultaev, B.; Dzhunusbekov, E.; Yestemessova, G.; Yelemanova, A. A novel regenerative snubber circuit for flyback topology converters. *J. Vibroeng.* **2020**, *22*, 983–992. [[CrossRef](#)]
10. Yoo, J.-S.; Baek, J.-O.; Ahn, T.-Y. A High-Efficiency QR Flyback DC–DC Converter with Reduced Switch Voltage Stress Realized by Applying a Self-Driven Active Snubber (SDAS). *Energies* **2023**, *16*, 1068. [[CrossRef](#)]
11. Tadvin, S.M.; Shah, S.R.B.; Hossain, M.R.T. A Brief Review of Snubber Circuits for Flyback Converter. In Proceedings of the 2018 3rd International Conference for Convergence in Technology (I2CT), Pune, India, 6–8 April 2018; pp. 1–5. [[CrossRef](#)]
12. Ai, T.-H. A Novel Integrated Non-dissipative Snubber for Flyback Converter. In Proceedings of the IEEE ICSS2005 International Conference on Systems and Signals, Philadelphia, PA, USA, 18–23 March 2005; pp. 66–71.
13. Liao, C.S.; Smedley, K.M. Design of high efficiency flyback converter with energy regenerative snubber. In Proceedings of the 2008 Twenty-Third Annual IEEE Applied Power Electronics Conference and Exposition, Austin, TX, USA, 24–28 February 2008; pp. 796–800.
14. Abramovitz, A.; Liao, C.-S.; Smedley, K. State-Plane Analysis of Regenerative Snubber for Flyback Converters. *IEEE Trans. Power Electron.* **2013**, *28*, 5323–5332. [[CrossRef](#)]
15. Alganidi, A.; Moschopoulos, G. A Comparative Study of Two Passive Regenerative Snubbers for Flyback Converters. In Proceedings of the 2018 IEEE International Symposium on Circuits and Systems (ISCAS), 2018 IEEE International Symposium on Circuits and Systems (ISCAS), Florence, Italy, 27–30 May 2018; pp. 1–4. [[CrossRef](#)]
16. Lee, Y.S.; Siu, K.W.; Lin, B.T. Novel single-stage isolated power-factor-corrected power supplies with regenerative clamping. Proceedings of APEC 97—Applied Power Electronics Conference, Atlanta, GA, USA, 27 February 1997; Volume 1, pp. 259–265. [[CrossRef](#)]
17. Vartak, C.; Abramovitz, A.; Smedley, K.M. Analysis and Design of Energy Regenerative Snubber for Transformer Isolated Converters. *IEEE Trans. Power Electron.* **2014**, *29*, 6030–6040. [[CrossRef](#)]
18. Alganidi, A.; Kumar, A. PI Controller Tuning & Stability study of the Flyback Converter with an Energy Regenerative Snubber. In Proceedings of the 2019 IEEE Canadian Conference of Electrical and Computer Engineering (CCECE), Edmonton, AB, Canada, 5–8 May 2019; pp. 1–4. [[CrossRef](#)]
19. Kim, J.-W.; Lee, I.-O.; Moon, G.-W.; Park, K.-B. Series input parallel output interleaved flyback converter with regenerative leakage inductance energy. In Proceedings of the 7th International Power Electronics and Motion Control Conference, Harbin, China, 2–5 June 2012; pp. 1347–1352. [[CrossRef](#)]
20. Scrimizzi, F.; Cammarata, F.; D’Agata, G.; Nicolosi, G.; Musumeci, S.; Rizzo, S.A. The GaN Breakthrough for Sustainable and Cost-Effective Mobility Electrification and Digitalization. *Electronics* **2023**, *12*, 1436. [[CrossRef](#)]
21. Cacciotto, F.; Cannone, A. Exploit GaN FET technologies in high efficiency flyback topologies: Pros and cons of different architectures. In Proceedings of the 2020 AEIT International Annual Conference (AEIT), Catania, Italy, 23–25 September 2020; pp. 1–6. [[CrossRef](#)]

22. Bohra, S.; Sarkar, A.; Anand, S. Low Side Switch Based Regenerative Snubber Circuit for Flyback Converter. In Proceedings of the 2020 IEEE Energy Conversion Congress and Exposition (ECCE), Detroit, MI, USA, 11–15 October 2020; pp. 4802–4807. [[CrossRef](#)]
23. Yau, Y.-T.; Hung, T.-L. Lossless Snubber for GaN-Based Flyback Converter with Common Mode Noise Consideration. *IEEE Access* **2022**, *10*, 56652–56667. [[CrossRef](#)]

**Disclaimer/Publisher’s Note:** The statements, opinions and data contained in all publications are solely those of the individual author(s) and contributor(s) and not of MDPI and/or the editor(s). MDPI and/or the editor(s) disclaim responsibility for any injury to people or property resulting from any ideas, methods, instructions or products referred to in the content.